5-14-2019

Synthesis of Novel RelII and ReV Metallointercalator Complexes for Use as DNA Damage Probes

Eli Schwartz
Bridgewater State University

Synthesis of Novel Re^{III} and Re^{V} Metallointercalator Complexes for Use as DNA Damage Probes

Eli Schwartz

Submitted in Partial Completion of the
Requirements for Commonwealth Honors in Chemistry

Bridgewater State University

May 14, 2019

Dr. Steven Haefner, Thesis Advisor
Dr. Thayaparan Paramanathan, Committee Member
Dr. Samer Lone, Committee Member

Acknowledgements

I would like to thank my thesis advisor Dr. Haefner first and foremost for his advice and mentorship throughout this project. I would also like to thank Drs. Thayaparan Paramanathan and Sam Lone for being my thesis committee members, as well as the Adrian Tinsley Program for providing me a grant with which to conduct summer research, and the Office of Undergraduate research at Bridgewater State University for providing me the opportunity to present this research at the 257th American Chemical Society National Meeting in Orlando, FL. Finally, I would like to thank Drs. Ed Brush, Stephen Waratuke, and Sarah Soltau, as well as Barbara Schwartz, Mark Schwartz, Alex Brown, Ashley Berube, Erica Hess, Brynna Turner, Jacqueline LaVallee, Cory Enos, Ryan Loughran, Jared Samost, Katherine Trudell, Allen Charest, Sara Ferreira, and Claire Martin for their unwavering support throughout this project.

Abstract

Cancer is a disease that affects millions around the globe. Treatments such as radiation and chemotherapy are often used to treat cancerous tumors, but are not 100% effective in curing the patient. Alternatively, some research groups have proposed the use of metallointercalators, metal complexes consisting of a rhodium, ruthenium, or iridium metal center with bidentate supporting ligands such as bipyridine and phenanthroline, or tridentate ligands such as terpyridine. The complexes also contain a bidentate intercalating group such as dipyridophenazine. These complexes possess the ability to directly bind to DNA through intercalation between the stacks of DNA base pairs, giving them the potential to be used as probes to analyze and identify chemically damaged DNA. The ultimate goal would be to design molecules that could detect damaged DNA at the molecular level and allow treatment before tumors could develop. Our objective is to design and synthesize novel metallointercalator complexes of rhenium, and to examine their physical and spectroscopic properties. Specifically, we are attempting to prepare $[Re(Py_2NO)(dppz)L]^{3+}$, where L = H_2O or NH_3. (Py_2NO = 4,4-dimethyl-2,2-di(2-pyridyl)oxazolidine; dpk-OEt = $(py)_2C(O)OCH_2CH_3$; dppz = dipyridophenazine). Reaction of $TBA_2[Re_2Cl_8]$ with the nitroxide ligand Py_2NO in acetonitrile produces a red/brown compound proposed to be $Re(Py_2NO)Cl_3$. Isolation and purification of this compound has proven to be a challenge. NMR studies indicate the compound is present as an intractable mixture. When the same reaction is performed in ethanol, the blue complex ReO(dpk-OEt)Cl_2 is obtained. The same compound can be isolated in good yield by direct reaction of two equivalents of di-2-pyridyl ketone with $TBA_2[Re_2Cl_8]$. The blue complex has been reacted with two equivalents of Ag^+ followed by the addition of dppz to produce a brown solid believed to be the metallointercalator $[ReO(dpk\text{-}OEt)dppz]^{2+}$. Details of the synthesis along with IR, NMR, and UV/Vis spectral characterization of these compounds are described.

Introduction

Deoxyribonucleic acid (DNA) is the molecule responsible for holding all of the genetic information of every cell in every living organism on the planet. DNA is a polymer which can come in various lengths, depending on the amount of information required to facilitate the proper function of a cell. This information is stored in the form of four primary bases: Adenine (A), Thymine (T), Cytosine (C), and Guanine (G). In a structure of DNA (Fig. 1), these bases are found in pairs: A pairs with T, and C pairs with G. The pairs are held together by weak

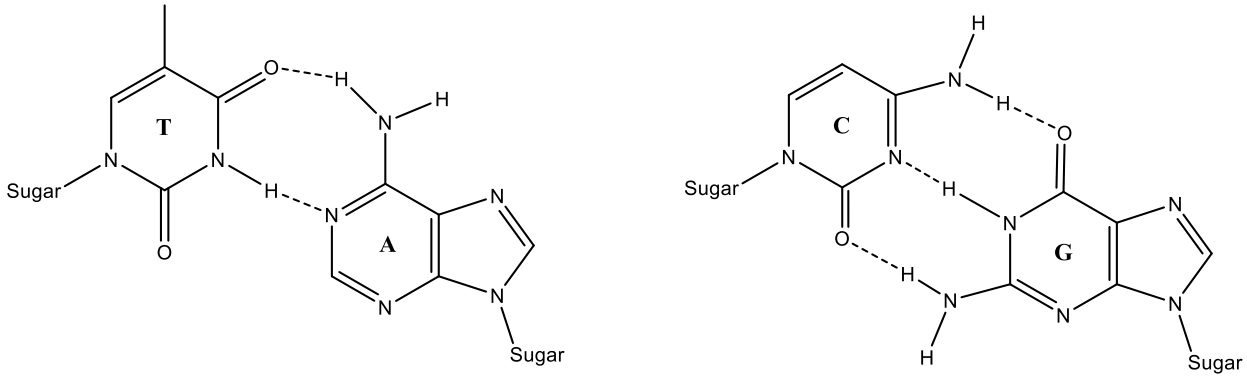

Figure 1: Molecular structure of A-T and C-G DNA base pairs.

interactions known as hydrogen bonds, which become extremely strong when combined in a group, similar to a bundle of twigs.[1] This stacking nature of DNA bases allows for DNA's well-known double-helix structure, which is maintained by the bases attaching to a negatively charged sugar-phosphate backbone.[2]

DNA bases repeat in various orders throughout a molecule or sequence of DNA. The order in which these bases appear in a sequence encodes the genetic information held in a cell. The DNA can then be read by other molecules within a cell, and translated into what the base sequences code for: proteins. In other words, the order of bases in a DNA sequence dictates how

a specific protein is to be constructed. This properly constructed protein can then carry out a task which helps to keep the cell functioning properly.[2]

Since DNA codes for proteins, which have an overwhelming diversity of structure and function within cells and organisms, it is extremely important to ensure the DNA sequences that code for these proteins remain the same. If even one base is altered or mutated, the structure and function of the sequence's corresponding protein can be affected.[2] Some of the consequences of this can include a protein whose creation was terminated prematurely, or a protein containing the wrong amino acids. Both of these scenarios can prevent the protein from functioning properly in the cell, because it does not have the proper structure to carry out its function. This lack of function can in turn lead to diseases such as cancer.[3]

Over time, an organism's DNA can accumulate multiple mutations as well as chemical modifications. These can result in proteins being formed improperly, as the genetic information that codes for the protein is either mutated or disrupted due to DNA damage. Thus, proteins may not function properly due to their improper structure, which can have catastrophic consequences for both a cell and an organism.

Fortunately, the human body has a mechanism to solve the problem of DNA mismatches: mismatch repair (MMR) machinery. The DNA mismatch repair machinery consists of enzymes that recognize and repair DNA mismatches, reducing their frequency by a factor of 1000.[4–6] As with other aspects in the genome, however, there can be mutations in the MMR genes, known as MMR deficiencies. MMR deficiencies increase the amount of unchecked DNA mutations, which can result in an increased risk for developing cancers.[6] To add insult to injury, it has been shown that MMR deficiencies are associated with an increased tolerance to traditional chemotherapeutics such as cisplatin, carboplatin, doxorubicin, and mercaptopurine.[5,7] MMR

deficiencies are therefore a high-priority target for cancer recognition treatment. There are other mechanisms in cells to repair DNA damage, known as lesions, which work similarly to the mismatch repair machinery. Like MMR deficiencies, deficiencies in the DNA lesion repair genes can lead to increased DNA damage in cells, and thus a higher risk for developing cancer.

One proposed treatment solution to cancer and other genetic disorders is DNA repair. Disorders such as cancers, Huntington's disease, cystic fibrosis, sickle cell anemia, and even Alzheimer's and Parkinson's diseases have been linked to missing, mismatched, or chemically damaged DNA.[3] The way to treat these diseases would be to treat them at the smallest level possible: repairing or replacing the damaged or missing DNA sequence to reflect the complete, undamaged sequence. Consequently, the cell would now be able to properly carry out its function by synthesizing the complete protein required to carry out the function that the cell was previously unable to do. Repairing MMR deficiencies would be advantageous as well, as the cell would then be able to perform gene repair without outside assistance.

In order to repair damaged DNA, it must be found. Thus, molecules that can selectively recognize and bind to DNA would be highly valuable. One such class of molecules, known as metallointercalators, has been shown to act as a DNA probe with some success. A metallointercalator, as shown by Figure 2, is a metal complex which contains a metal center, one or more supporting ligands, and an intercalating group.

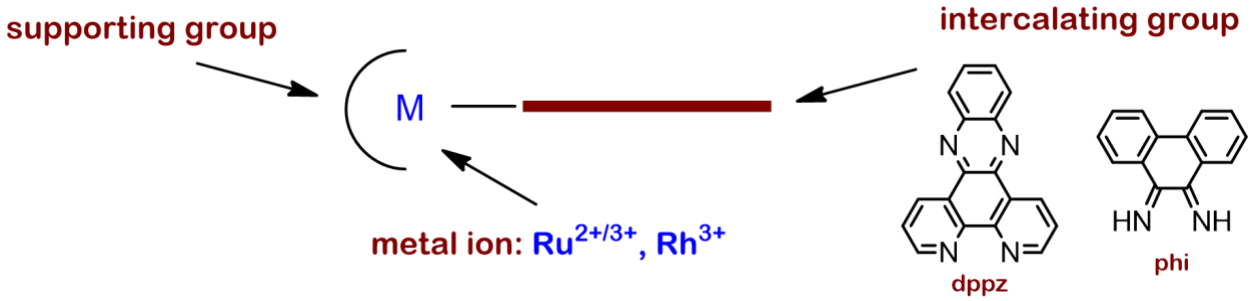

Figure 2: Diagram of a general metallointercalator complex, showing the metal ion, supporting group, and intercalating group.

The binding mode of a metallointercalator complex to DNA consists of three components, which work in concert: the first, and typically strongest, binding component is an electrostatic interaction between the positively-charged metal complex and the negatively-charged sugar-phosphate backbone of DNA. The second component consists of aromatic pi-stacking interactions between the aromatic, hydrophobic intercalating group and the aromatic DNA base pairs. Finally, hydrogen bond interactions can take place between the capping ligand or ancillary groups on the metallointercalator complex and the hydrogen bond donors and acceptors on the sugar-phosphate backbone of DNA. This provides added stability for the complex when bound to DNA, and can be used to recognize specific base pair sequences.

The metal ion is the centerpiece of the metallointercalator complex. Acting as a foundation, the metal center is the site to which the supporting ligand, intercalating group, and ancillary groups coordinate. The metal center also provides the complex with a net positive charge. A more positively-charged metal center allows for a stronger electrostatic interaction between the positively-charged metallointercalator and the negatively-charged DNA backbone. The most extensively used metal centers for these complexes have traditionally been Rh^{III} and $Ru^{II/III}$.[8] These metals possess low spin d^5 and d^6 configurations which renders them inert with respect to ligand substitution or exchange.[8]

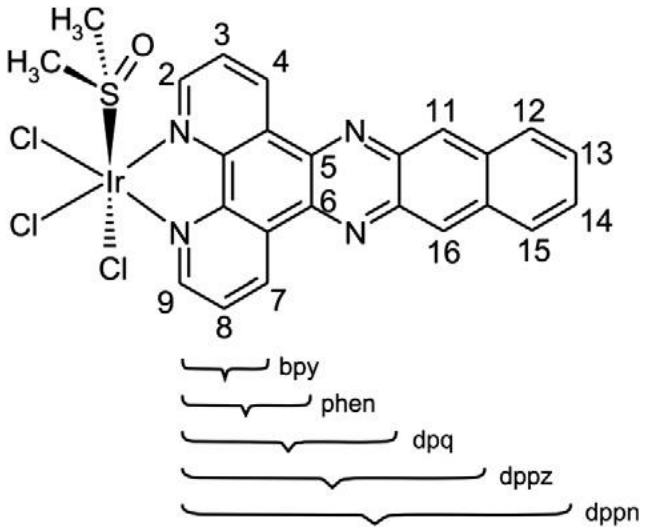

Figure 3: Diagram of an iridium metallointercalator complex highlighting the possible variation in polypyridyl intercalating groups. Bipyridine, phenanthroline, dpq, dppz, and dppn are shown.[21]

The intercalating group is the ligand which inserts between the DNA base pairs, similar to sliding between the rungs of a ladder. Intercalating groups are planar, hydrophobic, aromatic, organic compounds consisting of three to five or more rings. Most intercalating groups are bidentate, coordinating to the metal center through two nitrogen atoms. Common examples are dipyridophenazine (dppz), a conjugated five-ring system containing four nitrogen atoms, two of which coordinate to the metal center, as well as phi, a conjugated three-ring system that coordinates to the metal center through two nitrogen atoms (Fig. 2). Figure 3 shows the possible variation in polypyridyl intercalating groups like dppz, highlighting the ability to adjust the length of the intercalator. When bound to DNA, intercalating groups exhibit both hydrophobic and pi-stacking interactions with the DNA base pairs, contributing to the stability of the metallointercalator-DNA complex as a whole.

One important property of several metallointercalator complexes is their ability to emit light upon intercalation, otherwise known as “light-switch complexes”. One such complex is

$[Ru(bpy)_2(dppz)]^{2+}$ (bpy = bipyridine), shown in Figure 4. This metal complex does not fluoresce when by itself in aqueous solution, but when bound to DNA, the complex emits red light.[9] This is due to water hydrogen bonding to the nitrogen atoms of dppz when in solution, preventing the emission of light. When interacting with DNA, however, dppz is intercalated between the base pairs in the hydrophobic region of DNA. Thus, water is unable to hydrogen bond with dppz's nitrogen atoms, allowing for light emission.[9] This unique property has the potential to be applied to other metallointercalator complexes, possibly allowing for differing fluorescent properties based on the substituent and supporting groups bound to the metal ion center.

Many of the known light-switch complexes are Ru-dppz based intercalators. Another intercalator variation, based on Rh-phi, has demonstrated the ability to cleave DNA strands when exposed to UV light in the 313-325 nm range.[10,11] Two examples of these photocleaving metallointercalators are $[Rh(phen)_2(phi)]^{3+}$ and $[Rh(phi)_2(bpy)]^{3+}$ (Fig. 5). In addition, it has

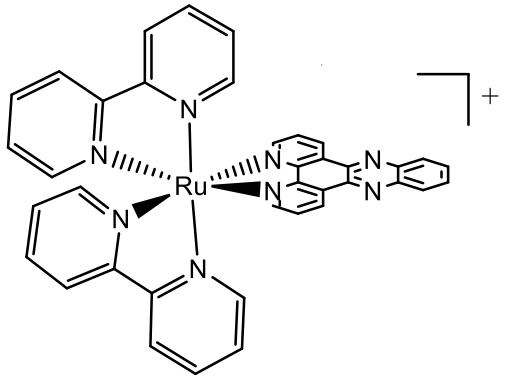

Figure 4: Chemical structure of the light-switch complex $[Ru(bpy)_2(dppz)]^{2+}$.[9]

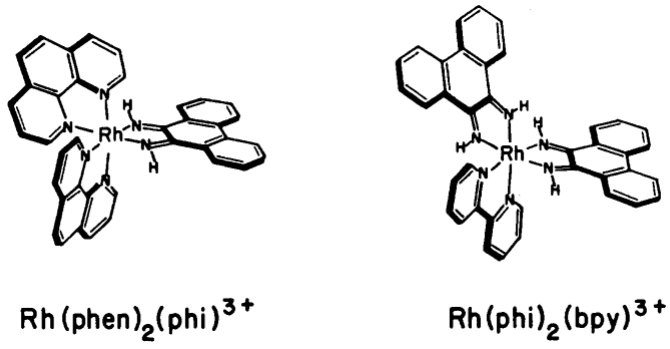

Figure 5: Chemical structures of two Rh-phi metallointercalator complexes, $[Ru(phen)_2(phi)]^{3+}$ and $[Rh(phi)_2(bpy)]^{3+}$, with the ability to photocleave DNA. The mode of DNA recognition, binding, and cleavage is dependent on the structure of the metal complexes.[11]

been discovered that the shape of these complexes dictates their method of DNA recognition and cleavage. In other words, the shape of each complex, or the way it is designed, changes how the complex recognizes, binds to, and cleaves the DNA strand.[11]

Although extensive work has been conducted in the synthesis and characterization of rhodium and ruthenium metallointercalators, rhenium-based metallointercalator complexes are largely unknown. To date, there has been one known report of a Re^{I}-dppz complex used as a metallointercalator[12]: $[Re(CO)_3(4\text{-MePy})dppz]^+$ (4-MePy = 4-methylpyridine), shown by Figure

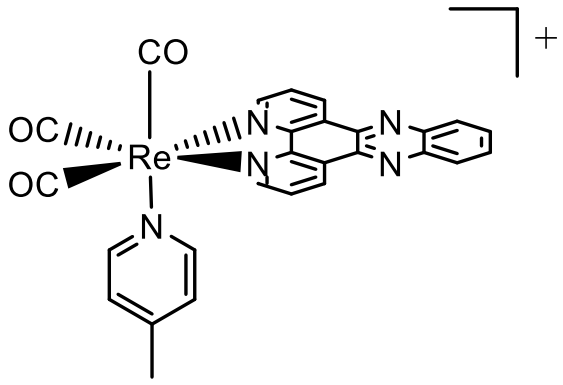

Figure 6: Chemical structure of the first reported rhenium-based metallointercalator complex: $[Re(CO)_3(4\text{-MePy})dppz]^+$.[12]

6. This complex was shown to intercalate into DNA, and like the Ru^{II} complexes previously mentioned, the complex exhibited fluorescence upon intercalation.[12] It has also been found that Re^{I} intercalators possess the ability to photocleave DNA.[13]

Further research was conducted with essentially the same complex, $[Re(CO)_3(Py)dppz]^+$, where 4-methylpyridine was substituted with pyridine (Py). During their research into amyloid beta peptide aggregation and its affects in Alzheimer's disease, Martí et al. discovered that $[Re(CO)_3(Py)dppz]^+$ also exhibits fluorescence in the presence of amyloid beta, in addition to DNA.[14]

Some research groups have worked with metalloinsertors, rather than metallointercalators, and it is important to highlight this distinction. A metallointercalator is a complex whose planar substituent group intercalates into, or inserts between, DNA base pairs. The DNA must stretch (which increases its viscosity) in order to accommodate the intercalating substituent of the metal complex, however the DNA strand remains intact.[8,15] Conversely, metalloinsertors interact with DNA in a way that results in the ejection of one or more bases from a strand of DNA.[10] This can be advantageous, as Barton et al. discuss the ability of the metalloinsertor $[Rh(bpy)_2(chrysi)]^{3+}$ to eject DNA mismatches, resulting in recognizable DNA lesions which have been shown to cause selective cell death of MMR-deficient cells, but not MMR-proficient cells.[15]

Despite their differences, parallels can be drawn between metallointercalators and metalloinsertors, and lessons can be learned in the design and application of metallointercalators. Barton et al. reported in 2011 that rhodium-based metalloinsertors cause necrosis in MMR-deficient cells. This is interesting, as cancer treatment has traditionally centered on inducing

apoptosis, or programmed cell death, in a cancer cell. Unlike apoptosis, necrosis is cell death resulting from causes outside the cell, such as injury or lack of blood flow.[6]

Barton et al. further suggest necrosis as a pathway to cancer treatment, as necrosis releases cytokines, an agent in the inflammatory response. They argue that this inflammatory response would allow the immune system to then selectively target and eliminate the necrotic cancer cells.[6] Similarly, one effective design of a metallointercalator would be one which selectively targets DNA mutants and causes necrosis in cancer cells.

The supporting ligand is an organic scaffold which typically contains nitrogen and/or oxygen, and coordinates to the metal center through these atoms. The ligand can be either bidentate, tridentate, or tetradentate, and provides stability to the metal complex, coordinating to sites on the metal which would otherwise be unutilized. There are many forms a supporting ligand can take, however the general structure is based on either a carbon-nitrogen ring or a series of connected pyridine rings. Supporting ligands generally occupy four of the six coordination sites on the metal center, and can be composed of two identical bidentate ligands or a single tetradentate ligand. It is also important that these ligands are neutral or monoanionic in order to preserve the positive overall charge of the metal complex.

Some classic examples of supporting ligands are bipyridine (bpy), terpyridine (terpy), and phenanthroline (phen), as shown in Figure 7. Many examples of metallointercalator complexes mentioned herein contain two bpy or phen molecules, or derivatives thereof, acting as supporting ligands. This method allows the supporting ligands to occupy four of the metal center's coordination sites, leaving two sites available for a bidentate intercalating group. Bpy,

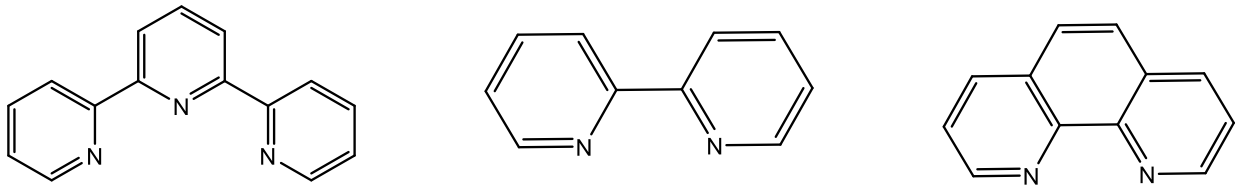

Figure 7: Terpyridine (left), bipyridine (center), and phenanthroline (right), classic examples of supporting ligands in metallointercalators with the inability to hydrogen bond.

phen, and terpy, however, are unable to hydrogen bond with the DNA backbone, as they lack hydrogen bond donors or acceptors. Furthermore, their only two hydrogen bond acceptors, both nitrogen atoms, are coordinated to the metal center. The lack of ability for these supporting ligands to hydrogen bond with the DNA backbone will consequently have an impact on the stability of the metallointercalator complex when bound to DNA.

There are, however, supporting ligands that contain hydrogen bond donors and acceptors, and are thus able to hydrogen bond with the DNA backbone. There are many advantages of this, some of which include additional stability of the metallointercalator when bound to DNA and the ability to fine tune the binding of the metallointercalator to specific DNA sequences.

Previous work by Jacqueline Barton et al. has demonstrated the ability of the metallointercalator complex Λ-1-Rh(MGP)$_2$phi^{5+} to be specific to the DNA sequence 5'-CATATG-3' (Fig. 8). The supporting group is able to hydrogen bond to the DNA backbone, providing the complex with increased stability. In addition, the metallointercalator bound competitively to the DNA sequence which is also bound by transcription factors for the gene following the sequence. Thus, the transcription factors were unable to bind to the DNA sequence, and were unable to dictate the synthesis of the protein that the gene following the sequence codes for.[16]

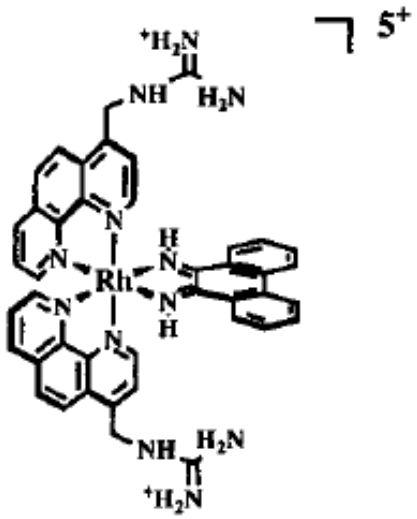

Figure 8: Molecular structure of Barton et al.'s DNA specific intercalator Λ-1-Rh(MGP)$_2$phi^{5+}. [16]

This gene-inhibiting property of a DNA sequence-specific metallointercalator could be advantageous. For example, if a sequence on a gene were damaged or mutated, a metallointercalator would be able to bind to the gene while the DNA sequence was repaired, preventing the cell from synthesizing a protein with an improper structure, which would not be able to carry out its necessary function. Once the DNA sequence was repaired, the metallointercalator would be removed from the DNA, allowing the cell to begin producing the

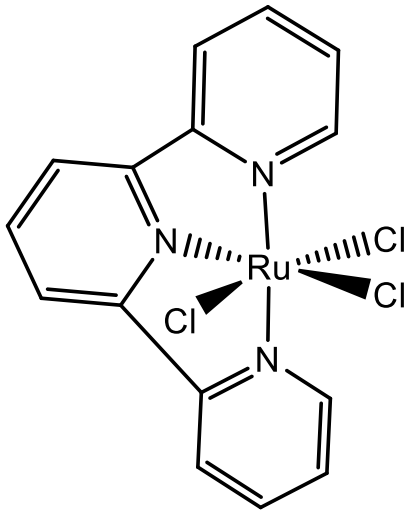

Figure 9: Chemical structure of the cytotoxic metal complex mer-[Ru(terpy)Cl₃]. This complex, which intercalates via the terpy ligand, demonstrates cytotoxicity and antitumor activity toward human cervix carcinoma cells.

protein which would now have a complete structure, rendering the protein fully functional once again.

Another metallointercalator produced by Barton et al. showed specificity for a single mismatch on a strand of DNA containing 2,725 base pairs.[17] Mismatches are ideal targets for metallointercalators because they are indicators of thermodynamic instability on a strand of DNA, due to their poor pi-stacking ability and loss of hydrogen bonding.[6]

In addition to showing sequence specificity, some metallointercalators have shown both cytotoxicity and antitumor activity. For example, *mer*-[Ru(terpy)Cl_3] (terpy = terpyridine) has shown cytotoxicity toward human cervix carcinoma cells *in vitro* (Fig. 9). In addition to cytotoxicity, this complex has demonstrated antitumor activity in the same cell line.[18]

Capping ligands are another option that can be used in lieu of supporting ligands. A capping ligand, unlike a supporting ligand, is tridentate. In binding to three of the metal's coordination sites instead of four, the capping ligand allows for an open binding site on the metal complex, which can be modified by coordinating various ancillary groups to the metal center.

This would further allow for modification of the metallointercalator's binding, reactive, and physical properties. Terpy is a classic example of a capping ligand. Like other supporting ligands, however, capping ligands with the ability to hydrogen bond with the DNA backbone would provide more stability to the metallointercalator and increased opportunity for sequence specificity.

As previously mentioned, capping ligands allow for the utilization of ancillary groups which coordinate to the metal center through an open binding site. These ancillary groups can be modified, thereby altering the behavior of the complex in solution, when it is bound to DNA, and can even inhibit intercalation.[8] Changing the ancillary group allows for control of the metal complex's physical and chemical properties such as hydrophobicity, binding affinity, sequence selectivity, and cellular uptake.[19] Greater control over the behavior of a metallointercalator translates to more efficient and more effective cancer treatments with fewer side effects. For example, some ancillary groups may provide the complex with a greater ability to hydrogen bond with the DNA backbone. Others may only interact with select DNA sequences, making some DNA sequences a specific target for the metallointercalator.

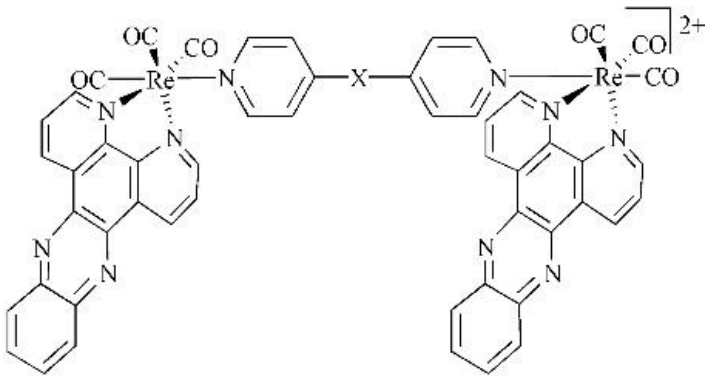

Figure 10: A general diagram showing a bi-metallointercalator system where two individual intercalators are linked by a linking molecule. An example is shown from Thomas et al. using the Re^{I} intercalator shown above.[13]

In addition to using the open binding site of the metallointercalator for ancillary groups, metallointercalators can be linked to one another through their open binding sites via a linking molecule (Fig. 10). Jim Thomas et al. have exploited this property using Re^{I}-dppz metal complexes, using the linkers 1,2-di(4-pyridyl)ethane (dpe) and 1,3-di(4-pyridyl)propane (dpp).[13] Sheldrick et al. have conducted similar studies with Ir-dppz complexes, using both pyrazine and 4,4'-bipyridine to link intercalators at the open binding site of the metal center.[20] In addition, Sheldrick et al. discuss cytotoxic chlororhodium^{III} complexes containing tridentate supporting ligands such as 1,4,7-trithiacyclononane and tris(pyrazolyl)methane (tpm).[21] These complexes allow for the coordination of a bidentate intercalating group such as dppz, and could then be linked together after substitution of the chlorine for any of the aforementioned linking molecules.

Previous Work

Previous work in the Haefner group has focused on using 1,4,7-triazacyclononane (tacn) as a capping ligand. Tacn is a tridentate capping ligand that allows for an open binding site on the metal center to which ancillary groups or linkers may bind. Unlike bpy, terpy, and phenanthroline, however, tacn contains three N-H groups, which have the ability to hydrogen bond to the DNA backbone. This hydrogen bonding ability of the capping ligand would provide the metallointercalator with an affinity for specific DNA sequences and more stability when bound to DNA.

The use of tacn in the Haefner group has been successful in metallointercalators containing a variety of metal centers, including Ru^{II}, Ir^{III}, and Rh^{III}. Previous examples include the metallointercalators $[Ru(tacn)(dppz)(DMSO)]^{2+}$, $[Ir(tacn)(dppz)(DMSO)]^{3+}$, $[Rh(tacn)(dppz)(H_2O)]^{3+}$ (Fig 11).[22–25] One of these metallointercalators,

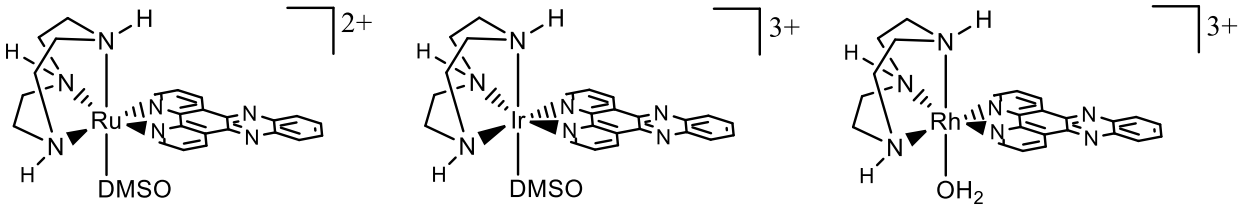

Figure 11: Three metallointercalator complexes containing the tacn capping ligand previously synthesized by the Haefner group. From left to right: [Ru(tacn)(dppz)(DMSO)]$^{2+}$, [Ir(tacn)(dppz)(DMSO)]$^{3+}$, [Rh(tacn)(dppz)(H$_2$O)]$^{3+}$.

[Rh(tacn)(dppz)(H$_2$O)][CF$_3$SO$_3$]$_3$, underwent preliminary DNA binding studies with calf-thymus DNA. Another DNA intercalator, ethidium bromide, was used as a fluorescence probe in the study. It was found that [Rh(tacn)(dppz)(H$_2$O)]$^{3+}$ replaced the ethidium bromide when it intercalated into DNA, resulting in the quenching of fluorescence, shown by Figure 12. This result indicated that [Rh(tacn)(dppz)(DMSO)]$^{3+}$ had a higher binding affinity to DNA than ethidium briomide.

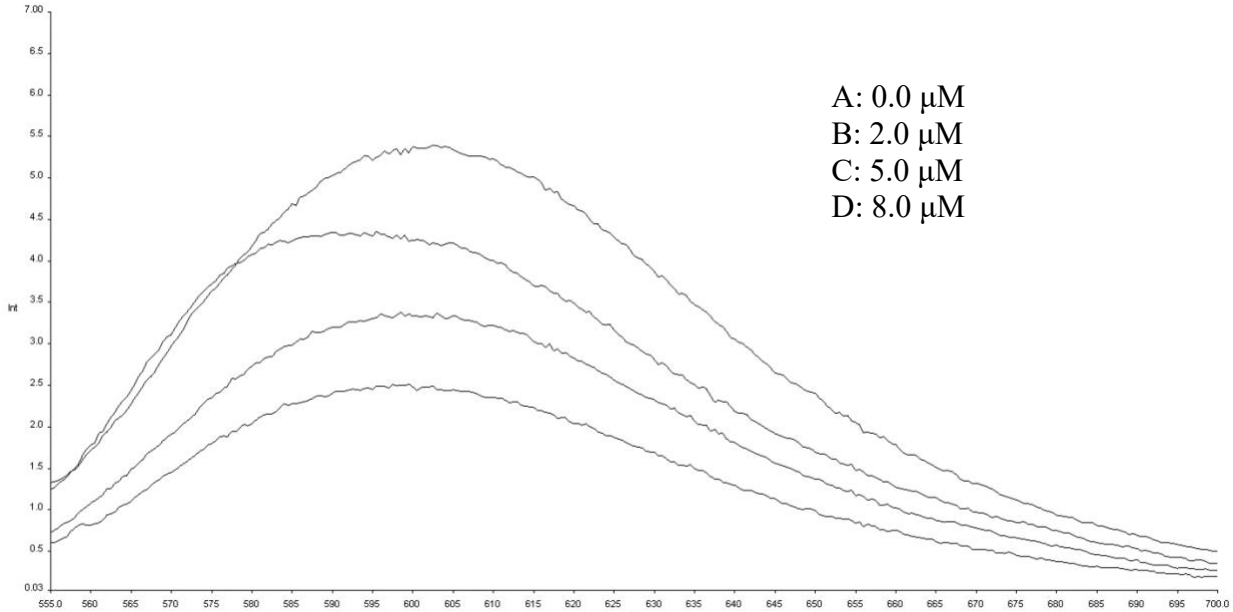

Figure 12: Absorption spectrum of DNA binding studies of [Rh(tacn)(dppz)(H$_2$O)]$^{3+}$with calf-thymus DNA using ethidium bromide as a fluorescence probe. Each curve corresponds to the fluorescence level with various concentrations of [Rh(tacn)(dppz)(H$_2$O)]$^{3+}$ ranging from 0 to 8 μM. Emission decreases with increasing concentration of [Rh(tacn)(dppz)(H$_2$O)]$^{3+}$.

Current Work

In an effort to develop new metallointercalators with different supporting groups, we began the examination of the tridentate ligand 4,4-dimethyl-2,2-di-2-pyridyl oxazolidine (Py_2NO). Previously, this capping ligand has been used to prepare first-row metal complexes with the general formula of $M(Py_2NO)_2^{n+}$, where M = Mn, Fe, Co, and Cu (Fig. 13).[26–29] These complexes were found to exhibit unusual magnetic properties including spin-crossover intermolecular ferromagnetic exchange and single molecule magnetism.[30]

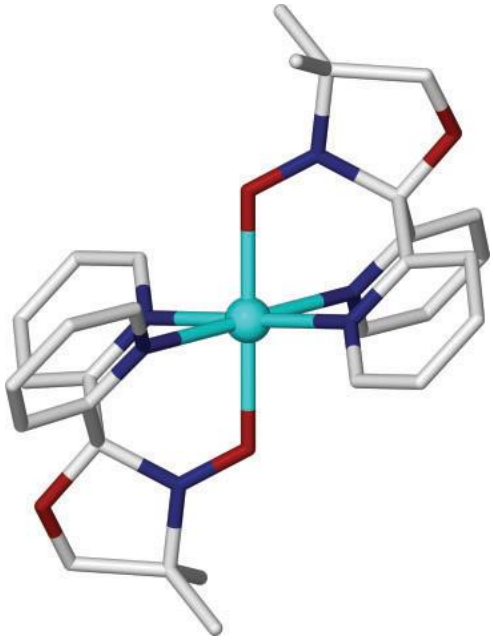

Figure 13: Molecular structure of $[Mn(Py_2NO)_2]^{2+}$, showing the tridentate nature of Py_2NO and its coordination behavior to the metal center. Murray et al. suggest that the Mn^{2+} ion is in a high-spin d^5 state, whereas our Re^{3+} ion is expected to be in a low-spin d^4 state, possibly suggesting a difference in behavior of these metal ions even though they reside in the same group.

Our interest in the ligand derives from its tridentate nature. Py_2NO would function as a capping ligand, making available the sixth coordination site of the metal center. Furthermore, the oxygen donor atom could act as a hydrogen bond acceptor, forming a hydrogen bond with the DNA backbone and thus providing more stability to the metallointercalator. Finally, the radical

nature of the hydroxide group could impart additional reactivity upon intercalation of the complex with DNA.

To date, there have been no reports of using Py_2NO to support second or third-row metal ions. We are particularly interested in using Py_2NO to develop new metallointercalator complexes of rhenium. As previously mentioned, metallointercalators of rhenium are relatively unknown, with the only reported Re-dppz metallointercalator having a charge of +1. Our target is the metallointercalator $[Re(Py_2NO)(dppz)H_2O]^{3+}$ (Fig. 15). This metallointercalator is novel in many ways, one of which is the utilization of the Re^{III} oxidation state instead of Re^{I}. The Py_2NO group will bind to the Re^{3+} ion through its two nitrogen atoms on the molecule's pyridine rings, as well as through a free radical oxygen which is part of a nitroxide on the oxazolidine ring. The dppz group will bind to the Re^{3+} ion through two of its nitrogen atoms. Figure 14 shows the open binding site, designated by "**L**", to which ancillary groups may bind.

This metallointercalator design has the potential to show various interesting properties. One such property, for example, is the ability to be tuned to bind to specific DNA sequences. Due to the complex's open binding site, this metallointercalator's physical and chemical properties will change, depending on the substituent bound to the open binding site of the complex. For example, some substituents may allow for increased hydrogen bonding between the metallointercalator complex and the DNA, thus allowing for more stability of the interaction

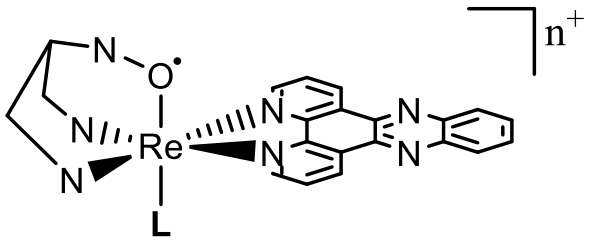

Figure 14: A diagram of one of our proposed metallointercalators. Emphasis is placed on the open binding site, designated by the bolded "L", which allows for the fine-tuning of the physical and chemical properties of the complex.

between the metallointercalator and the DNA. Conversely, another substituent may inhibit hydrogen bonding between the metal complex and the DNA at that or another specific site.

Another property that we expect this metallointercalator complex to exhibit is the ability to emit light when bound to DNA. As mentioned previously, some metallointercalator complexes containing dppz have been shown to fluoresce when bound to DNA, behaving as a "light switch". This property would facilitate the process of identifying DNA damage, reducing the time required for the DNA damage to be repaired.

Herein, we describe the synthesis and characterization of the metallointercalator intermediate $Re(Py_2NO)Cl_3$. We have also discovered another intermediate, $ReO(dpk\text{-}OEt)Cl_2$, a known complex which has been synthesized through a novel method in higher yield. A compound believed to be the metallointercalator $[ReO(dpk\text{-}OEt)dppz]^{2+}$ has been synthesized as well. The syntheses of these compounds, their physical and chemical properties, as well as data obtained from infrared spectroscopy, UV/Vis spectroscopy, and x-ray diffraction studies will be described.

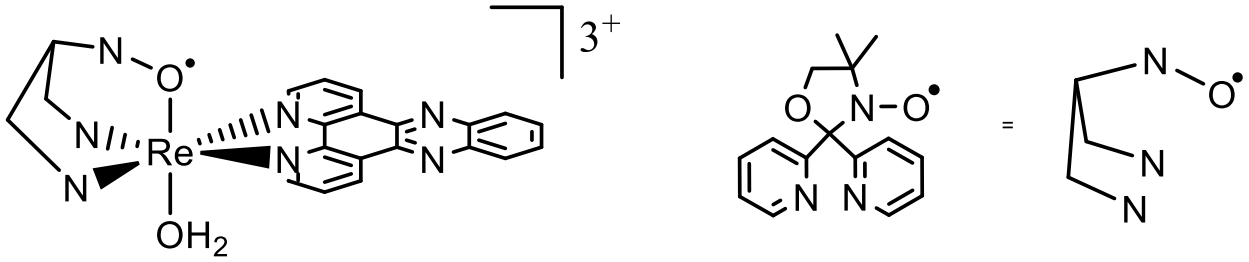

Figure 15: Chemical structure of one of our proposed novel metallointercalators: $[Re(Py_2NO)(H_2O)dppz]^{3+}$. A shorthand for Py_2NO is shown to the right of the structure.

Experimental Section

Materials and Methods. All reagents and solvents were purchased from commercial sources and used without further purification. Unless otherwise noted, all reactions were

conducted in an argon atmosphere using standard Schlenk line techniques. Work up of products was performed in air.

Characterization Techniques. Powders and crystals were analyzed by IR spectroscopy using a PerkinElmer® Frontier FT-IR/NIR Spectrometer. UV/Vis analysis was conducted using both a PerkinElmer® Lambda 25 UV/Vis Spectrometer and a Hewlett-Packard® Model 8453 diode array spectrometer in the solvents specified by the synthetic procedure. NMR spectral data was obtained using a JEOL 400 mHz spectrometer in deuterated solvents specified by the synthetic procedure. Chemical shifts were referenced using the known chemical shifts of the protio impurity in the deuterated solvent. X-ray diffraction studies were conducted by Dr. James Golen at the University of Massachusetts, Dartmouth. Data were collected at 24 ^{o}C on a Bruker D8 Venture X-ray instrument using Mo K alpha radiation and data were corrected for absorption with SADABS. Structure was solved by direct methods and all non-hydrogen atoms of main molecule were refined anisotropically by full matrix least squares on F^2. All hydrogen atoms were placed in calculated positions with appropriate riding parameters.

Synthetic Procedures.

4,4-dimethyl-2.2-di(2-pyridyl)oxazolidine (Py_2NO). Synthesis of Py_2NO was adapted from a literature procedure.[26] Di(2-pyridyl)ketone (9.71 g, 51.7 mmol), 2-amino-2-methylpropanol (110 mL, 1.13 mol), and concentrated sulfuric acid (25 drops) were added to 200 mL of toluene and refluxed for four days. The solution was then cooled to room temperature and concentrated. Water (200 mL) and diethyl ether (100 mL) were then added to the solution, forming aqueous and organic layers. The organic layer was separated, and the aqueous layer was

extracted twice with CH_2Cl_2 (100 mL). The organic layers were combined and dried with $MgSO_4$, and the solvents were evaporated, yielding an intermediate compound.[26]

The intermediate (3.01 g, 11.8 mmol) was mixed with diethyl ether (40 mL), and the solution was cooled on ice. Added to this solution was a solution containing meta-chloroperoxybenzoic acid (MCPBA, 4.34 g, 17.6 mmol) in 40 mL of diethyl ether. The reaction mixture was allowed to stand for four hours. A cold, 5% Na_2CO_3 solution (40 mL) was added to the reaction mixture to separate the aqueous and organic layers. The organic phase was extracted four times with the Na_2CO_3 solution (40 mL), while the aqueous phase was extracted five times with CH_2Cl_2 (40 mL). The organic phases were combined, washed twice with cold 5% Na_2CO_3 solution (40 mL), and dried with $MgSO_4$. The solvents were evaporated under vacuum, yielding an orange solid.[26] The orange solid was chromatographed on silica gel with acetone. Yield: 2.20 g (68%). IR (cm^{-1}): 3055 w, 2975 w, 2873 w, 1682 m, 1586 s, 1571 m, 1541 m, 1464 s, 1435 s, 1363 m, 1318 m, 1245 m, 1051 s, 992 s, 944 s, 775 s, 751 s. UV/Visible (CH_3CN; λ_{max}, nm): 260.

Tetrabutylammonium Octachlorodirhenate ($TBA_2[Re_2Cl_8]$). Synthesis of $TBA_2[Re_2Cl_8]$ was adapted from a literature procedure.[31] $TBA[ReO_4]$ (1.5 g, 3.04 mmol) was added to a 100 mL Schlenk flask, and the flask was filled with argon. Benzoyl chloride (15 mL, 129 mmol) was then syringed into the flask, resulting in a pale yellow solution, which changed in color from pale yellow to orange, red, and eventually dark green as the solution was heated. The flask was fitted with a reflux condenser and the solution was gently refluxed overnight (20-24 h). After 24 h, the reaction was cooled to room temperature, and a solution containing tetrabutylammonium bromide (2.5 g, 7.75 mmol), ethanol (35 mL), and concentrated aqueous hydrochloric acid (5 mL) was added to the reaction mixture. This solution was allowed to reflux

for an additional hour, after which it was cooled to room temperature and evaporated to roughly 25-30 mL using a rotary evaporator. The solution was then filtered through a 30 mL medium porosity sintered glass frit, and the resulting blue crystals were washed with 3 5-mL portions of ethanol, 10 mL of diethyl ether, and dried under vacuum.

The crude product was added to stirred, boiling methanol (50 mL) containing one drop of concentrated aqueous hydrochloric acid, then immediately filtered through a 30 mL medium porosity sintered glass frit into concentrated aqueous hydrochloric acid (50 mL). Some dark blue crystals precipitate at this stage and were isolated. Evaporation of the methanol via a rotary evaporator yields more crystals. Yield: 1.32 g (76%). IR (cm^{-1}): 2954 s, 2876 s, 1476 s, 1381 s, 1179 w, 1152 m, 1107 w, 1051 w, 1025 m, 879 s, 796 w, 736 s. UV/Visible (CH_3CN; λ_{max}, nm): 685.

Re(Py_2NO)Cl_3. $TBA_2[Re_2Cl_8]$ (100 mg, .088 mmol) and Py_2NO (47.4 mg, 0.175 mmol) were refluxed in CH_3CN (5 mL) in air for 24 hours. The acetonitrile was removed under vacuum, leaving a brown, oily product to which 10 mL each of acetone and hexane were added (1:1 volumetric ratio). The solvents were removed using a rotary evaporator, resulting in the formation of a red/brown solid which was washed with ethanol and filtered using a Hirsch funnel. IR (cm^{-1}): 3082 w, 2963 w, 2871 w, 1604 m, 1653 m, 1441 s, 1283 m, 1236 m, 1164 m, 1093 m, 1028 m, 965 m, 912 m, 766 s. UV/Visible (CH_3CN; λ_{max}, nm): 485, 272. ^1H NMR (400 MHz, CD_3CN, δ): 8.75 (t, 1H, py), 8.2 (q, 2H, py), 7.6 (d, 1H, py), 3.05 (s, 2H, $-CH_2$), 0.95 (s, 6H, $(-CH_3)_2$).

ReO(dpk-OEt)Cl_2 (Method A). $TBA_2[Re_2Cl_8]$ (100 mg, 0.088 mmol) and Py_2NO (47.4 mg, 0.175 mmol) were refluxed in ethanol (10 mL) under argon for 24 hours. The solution turned green upon addition of the ethanol, and became very dark within 15 minutes. A blue

precipitate formed after 24 hours, and was filtered using a Hirsch funnel and washed with diethyl ether. The solid was dissolved in methylene chloride, and the solvent was allowed to slowly evaporate. Dark blue crystals formed upon evaporation of the methylene chloride. Yield: 30 mg (34%). Infrared, UV-visible, and NMR spectroscopic data of the sample were also obtained. IR (cm^{-1}): 3073 w, 2978 w, 1601 m, 1438 m, 1280 m, 1233 s, 1218 m, 1170 m, 1120 w, 1093 m, 1045 m, 1007 m, 965 s, 953 m, 891 w, 805 m, 766 s, 698 s, 671 s. UV/Visible (CH_3CN; λ_{max}, nm): 342, 315, 249. ^{1}H NMR (400 MHz, $(CD_3)_2SO$, δ): 8.42 (d, 2H, py), 8.05 (q, 4H, py), 7.78 (t, 2H, py), 3.65 (q, 2H, -O*CH*$_2$CH$_3$), 1.30 (t, 3H, -OCH$_2$*CH*$_3$).

ReO(dpk-OEt)Cl$_2$ (Method B). TBA$_2$[Re$_2$Cl$_8$] (250 mg, 0.219 mmol) and di-2-pyridyl ketone (80.7 mg, 0.438 mmol) were refluxed in ethanol (10 mL) in air. The reaction proceeded as previously described, with the solution turning light green upon addition of ethanol and darker green within 15 minutes. A blue precipitate formed after 24 hours of reflux, and was filtered through a Hirsch funnel and washed with ethanol and diethyl ether. The crude product was dissolved in methylene chloride and filtered through a 5.75” inch glass pipet filter containing roughly 0.5 cm of Celite® into a 20 mL scintillation vial. The vial was then covered with Parafilm pierced with seven evenly distributed holes, and the solvent was allowed to slowly evaporate. Blue crystals formed upon evaporation of the solvent. Yield: 178 mg (81%).

[ReO(dpk-OEt)dppz]$^{2+}$. ReO(dpk-OEt)Cl$_2$ (50 mg, 0.995 mmol), silver trifluoromethanesulfonate (50.9 mg, 0.198 mmol), and dppz (28.6 mg, 0.101 mmol) were added to CH_3CN (5 mL) in a 50 mL round-bottomed flask. The solution was then gently refluxed in air for 24-28 hours. A gray/green precipitate formed and was filtered off using a Hirsch funnel. The resulting dark red filtrate was then pipet filtered through roughly 0.5 cm of Celite®. The solution was cooled on ice, and saturated aqueous potassium hexafluorophosphate was subsequently

added. The solution then appeared as a brown suspension as $[ReO(dpk\text{-}OEt)dppz][PF_6]_2$ precipitated. The red/brown precipitate was then isolated by filtration through a medium porosity sintered glass frit before being dried under vacuum. The compound believed to be $[ReO(dpk\text{-}OEt)dppz][PF_6]_2$ was then dissolved in acetone and the solution was pipet filtered through 0.5 cm of Celite®. In a 20 mL scintillation vial, 5 mL of this solution was layered with toluene (5 mL), and the acetone was allowed to evaporate. Small, cube-shaped, red-orange crystals formed. Yield: 83.7 mg (42%). IR (cm^{-1}): 3642 w, 3099 w, 1700 w, 1608 m, 1497 m, 1423 m, 1360 m, 1238 m, 1080 m, 1038 m, 957 m, 829 s, 763 s, 728 s. UV/Visible (CH_3CN; λ_{max}, nm): 374, 358, 277. ^1H NMR (400 MHz, CD_3CN, δ): 9.70 (d, 1H, py), 8.50 (q, 2H, dppz), 8.17 (q, 1H, py), 7.97 (d, 1H, dppz), 7.83 (t, 1H, py), 0.95 (t, 1H, $-OCH_2\mathit{CH_3}$).

Results and Discussion

Synthesis of Py_2NO

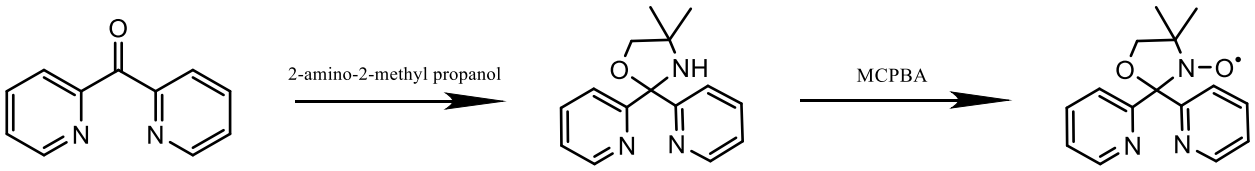

Figure 16: Chemical reaction of di-2-pyridyl ketone, 2-amino-2-methyl propanol, and MCPBA to produce the tridentate ligand Py_2NO.

The Py_2NO ligand was synthesized first by the reflux of di-2-pyridyl ketone, 2-amino-2-methyl propanol, and sulfuric acid in toluene (Fig. 16). The solution was a bronze color upon addition of the reagents. Upon quenching of the reaction, the solution appeared to be two layers, with a gold colored top layer and a smaller, cloudy layer on the bottom which contained some precipitate. The organic product was isolated from the aqueous byproduct, and this solution was

light amber in color. A crude, solid product was later obtained, and was light yellow in color with a chalky texture.

This crude product was then oxidized with 3-chloroperoxybenzoic acid (MCPBA) to produce the nitroxide product. The reaction mixture changed in color from green to yellow and eventually orange. The crude product was then chromatographed on silica gel with acetone, yielding the pure Py_2NO ligand.

Synthesis of $Re(Py_2NO)Cl_3$

Our initial objective was to react two equivalents of Py_2NO with the Re^{3+} precursor $[TBA]_2[Re_2Cl_8]$ in an effort to prepare the intermediate $Re(Py_2NO)Cl_3$ (Fig. 17). We then envisioned that removal of the halides followed by addition of dppz would lead to the new rhenium-based metallointercalator $[Re(Py_2NO)(dppz)L]^{3+}$ (L = CH_3CN or H_2O). Reaction of Py_2NO with $[TBA]_2[Re_2Cl_8]$ under reflux with CH_3CN in air produced a dark red/brown solution. Similar results were obtained under reflux conditions, as well as in other aprotic solvents such as acetone. Removal of the solvent under vacuum consistently produced an oily, intractable solid. We found that a red/brown precipitate could be obtained by the slow addition of equal volume of hexane to acetone solutions of the product, which were then evaporated under vacuum. The crude, red/brown solid compound was soluble in polar aprotic solvents, specifically acetone, acetonitrile, and methylene chloride.

An IR spectrum of the crude solid exhibited vibrations similar to that of free Py_2NO but shifted from 0 to 30 cm^{-1}, strongly suggesting coordination of the ligand to the rhenium metal center. The electronic absorption spectrum of the solid contained absorbances at 485 and 272 nm. The $Re_2Cl_8^{2-}$ δ-δ^* transition at 685 nm, however, was absent, indicating that cleavage of the Re-Re quadruple bond had occurred.

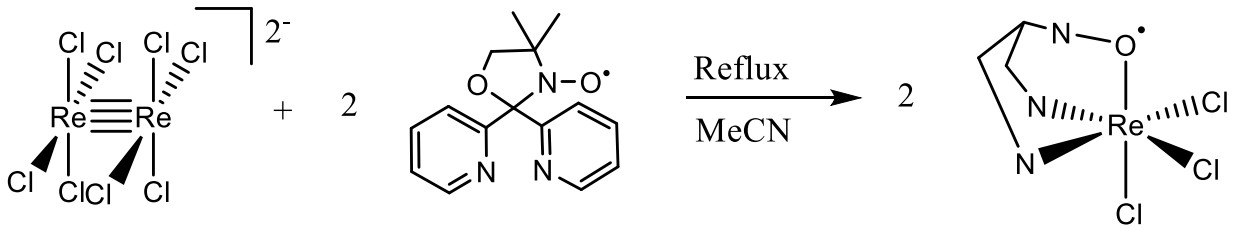

Figure 17: Chemical reaction of $TBA_2[Re_2Cl_8]$ and Py_2NO in acetonitrile to produce the intermediate $Re(Py_2NO)Cl_3$.

The ^1H NMR spectrum of the solid (Fig. 18) revealed a complex set of broad resonances in the aromatic region. The broadness of the resonances is indicative of a paramagnetic species. Cleavage of the Re-Re quadruple bond would produce a mononuclear Re^{3+}, low spin d^4 center that would be expected to be paramagnetic. It appears as though there are two sets of aromatic resonances. The first set consists of broad resonances at 8.75, 8.2, and 7.6 ppm. This would be consistent with a symmetric $Re(Py_2NO)$ species such as $Re(Py_2NO)Cl_3$, where the two pyridyl groups would be equivalent. There is also a more intense resonance at 1.0 ppm which integrates for roughly seven protons. This resonance corresponds to the dimethyl group on the oxazolidine ring. The methylene protons of the ring appear at 3.0 ppm. The second set of resonances in the aromatic region are more numerous and suggest a Py_2NO complex that lacks mirror symmetry, thus making the pyridyl rings inequivalent. Similar resonances appear upfield in the methyl and methylene regions.

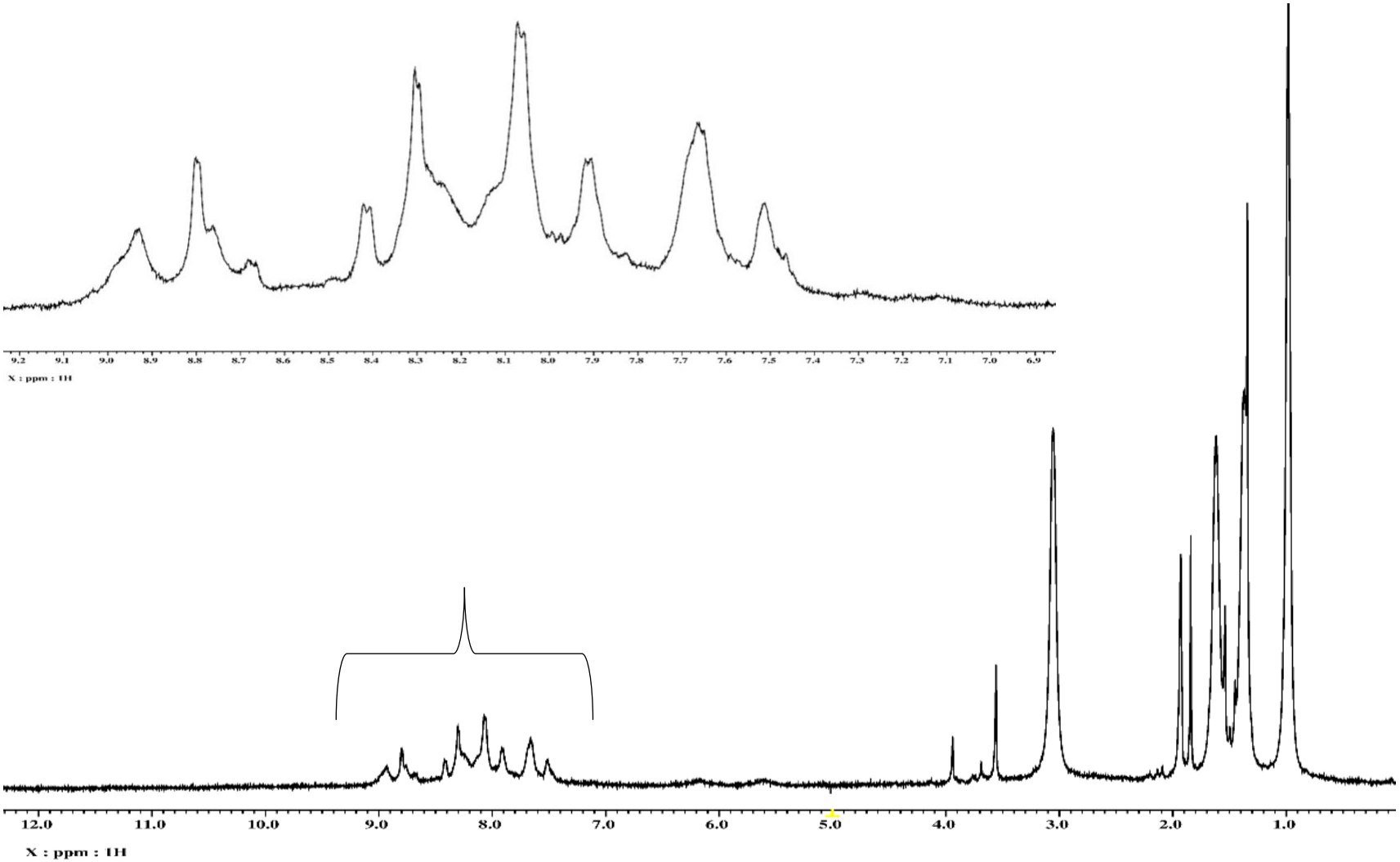

Figure 18: NMR Spectrum showing the metal complex believed to be $Re(Py_2NO)Cl_3$ in deuterated acetonitrile. The enlarged aromatic region (9-7ppm) suggests coordination of Py_2NO with the metal complex. We also expected this complex to be paramagnetic. The broadness of the aromatic peaks suggests that the complex may be paramagnetic, possibly providing further evidence of the identity of this metal complex as $Re(Py_2NO)Cl_3$.

Unfortunately, attempts to obtain single crystals of the intermediate $Re(Py_2NO)Cl_3$ have been unsuccessful, and further studies will need to be conducted in order to properly characterize this complex as $Re(Py_2NO)Cl_3$. The yields of this product were very low, and were insufficient for the synthesis of the metallointercalator $[Re(Py_2NO)(dppz)H_2O]^{3+}$. It is important to note that since the complex is expected to be paramagnetic, the exact oxidation state of the metal will be complicated by the presence of the nitroxide radical of Py_2NO. Regardless of the metal oxidation state, however, that the overall charge of the complex should remain 3+.

Synthesis of $ReO(dpk\text{-}OEt)Cl_2$

Surprisingly, the reaction between $TBA_2[Re_2Cl_8]$ and Py_2NO in alcohols such as ethanol under argon resulted in the precipitation of a blue solid (Fig. 19). Single crystals of this blue complex were obtained by dissolution in and slow evaporation of methylene chloride. An x-ray

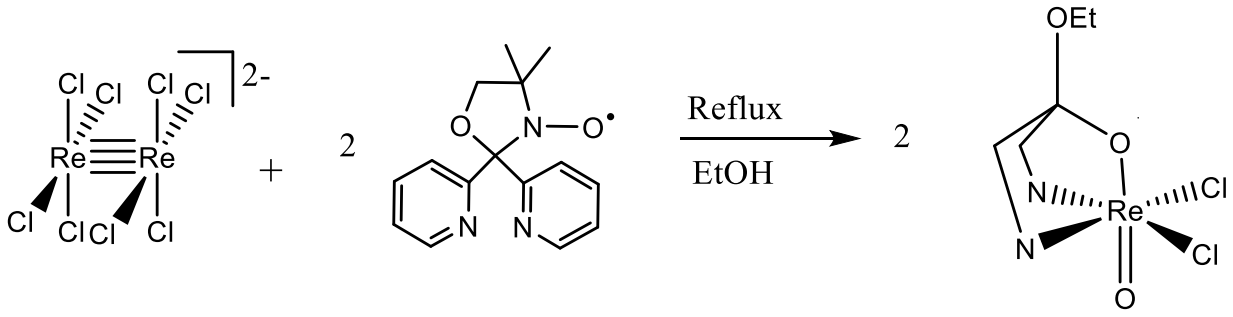

Figure 19: Chemical reaction of $TBA_2[Re_2Cl_8]$ and Py_2NO in ethanol to produce the intermediate $ReO(dpk\text{-}OEt)Cl_2$.

diffraction study on the compound revealed it to be the Re^V oxo complex $ReO(dpk\text{-}OEt)Cl_2$. Apparently, this reaction results in the decomposition of the Py_2NO ligand to reform di-2-pyridyl ketone, which then reacts with ethanol to form the dpk-OEt ligand. While the origin of the Re^V oxo is unknown, it appears likely to be derived from the nitroxide oxygen of the Py_2NO. Transfer of the oxygen to the rhenium metal center facilitates further decomposition of Py_2NO. Additional

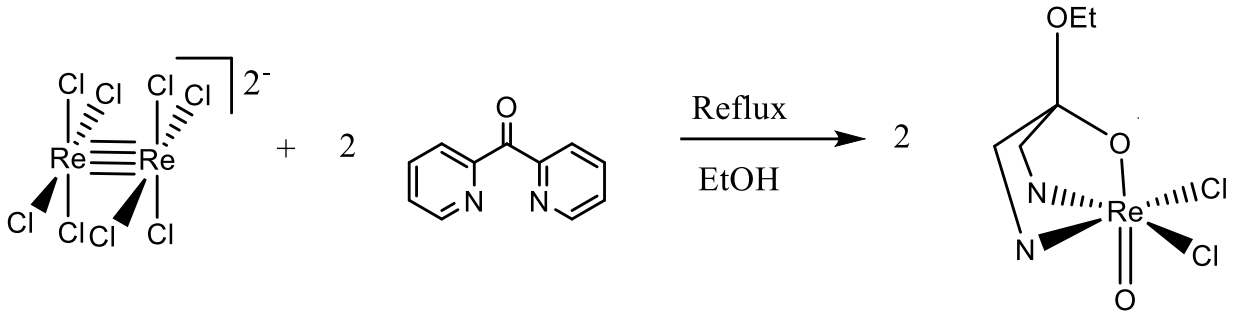

Figure 20: Chemical reaction of $TBA_2[Re_2Cl_8]$ and di-2-pyridyl ketone in ethanol to produce the intermediate $ReO(dpk\text{-}OEt)Cl_2$.

studies are required to identify the source of the oxo group and the decomposition byproducts of the Py_2NO ligand.

This Re^V oxo sample can be prepared in much higher yield through the direct reaction of $TBA_2[Re_2Cl_8]$ with di-2-pyridyl ketone in ethanol in air (Fig. 20). In fact, the yield for $ReO(dpk\text{-}OEt)Cl_2$ using $TBA_2[Re_2Cl_8]$ is higher than that previously reported by Gonzàlez et al. using $TBA[ReCl_5(DMF)]$ as a precursor.[32] A proposed mechanism of this reaction is shown by Figure 21, which suggests that coordination of the nitrogen atoms to the metal activates the carbonyl carbon of di-2-pyridyl ketone. Ethanol acts as a nucleophile, attacking the carbonyl carbon which then produces the dpk-OEt ligand.

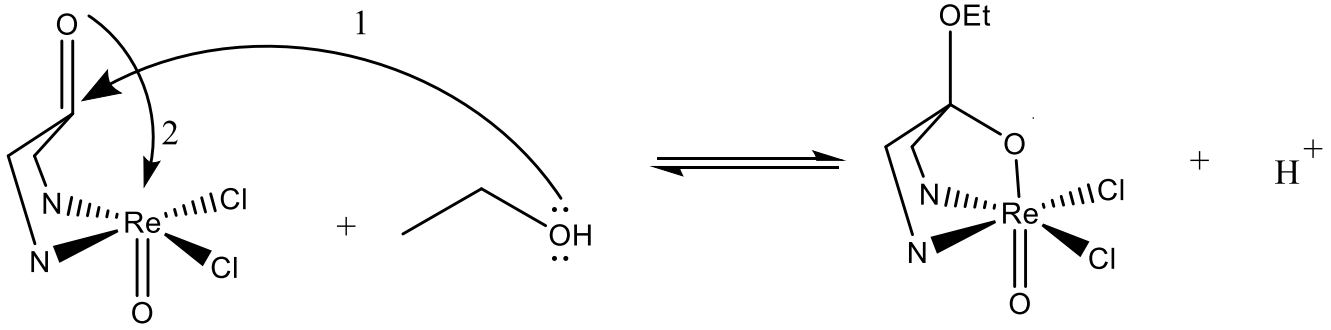

Figure 21: Proposed mechanism of the formation of the dpk-OEt. Metal coordination activates the carbonyl carbon of the di-2-pyridyl ketone, causing the reversible addition of ethanol acting as a nucleophile.

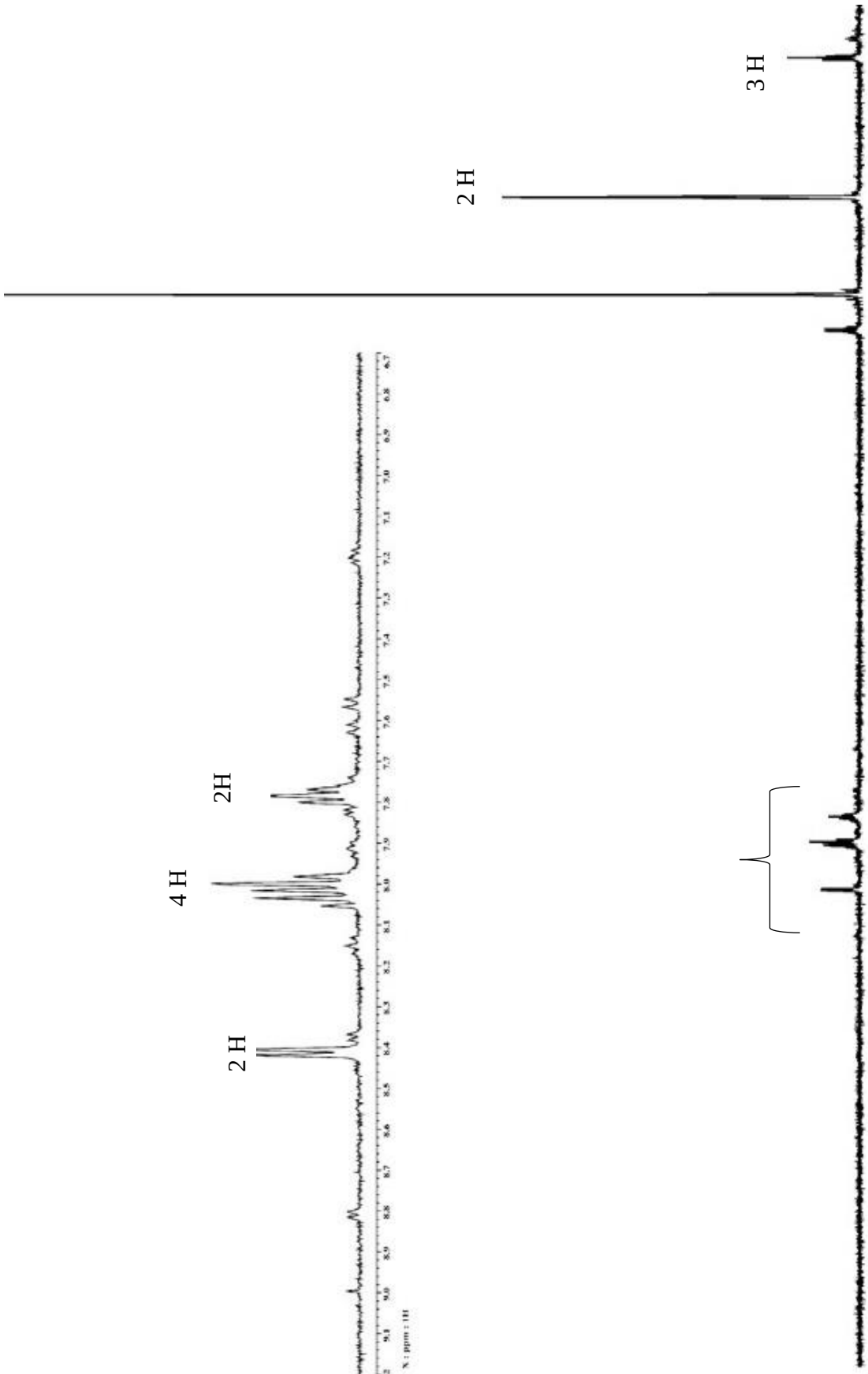

Figure 22: NMR spectrum of ReO(dpk-OEt)Cl_2 (with integration) in deuterated DMSO. The enlarged aromatic region (9-7ppm) shows the splitting of the pyridine rings associated with the metal complex. The fact that the splitting is not duplicated suggests that this metal complex has a plane of symmetry, which is confirmed by analysis if the crystal structure.

The electronic absorption spectrum of $ReO(dpk\text{-}OEt)Cl_2$ showed absorbances at 342, 315, and 249 nm, which indicates both the cleavage of the Re-Re quadruple bond as the δ-δ* transition at 685 nm is absent, and the coordination of the dpk-OEt ligand to the rhenium metal center. The IR spectrum exhibits absorptions consistent with the coordination of the dpk-OEt ligand to the rhenium center. In addition, the strong absorbance at 965 cm^{-1} corresponds to the Re=O stretch, also reported at 965 cm^{-1} by Gonzàlez et al.[32] The ^1H NMR spectrum (Fig. 22)

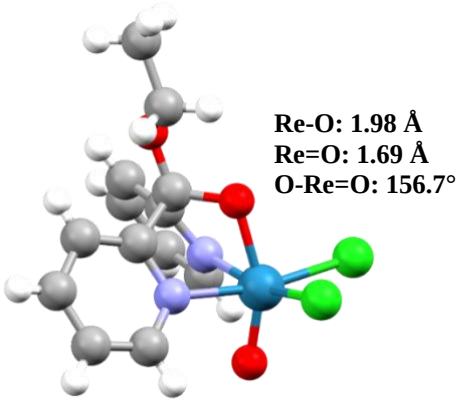

*Figure 23: X-ray crystal structure showing $ReO(dpk\text{-}OEt)Cl_2$. Rhenium, Oxygen, Chlorine, Nitrogen, Carbon, Hydrogen (White). (Gonzàlez, et al. **2011**).*

shows three major resonances in the aromatic region between 7.5 and 8.5 ppm, which would be consistent with the expectation of $ReO(dpk\text{-}OEt)Cl_2$ being a symmetric species. The quartet at 8.0 ppm is suggestive of proton coupling occurring within the pyridine rings, which would be confirmed by future 2-D NMR experiments such as COSY and HMQC. The upfield resonances at 3.65 ppm and 1.30 ppm correspond to the CH_2 and CH_3 protons on the ethoxyl group, respectively. The diamagnetic nature of this low spin d^2 center suggests the two d-electrons occupy the same molecular orbital, highlighting the labile nature of the $ReO(dpk\text{-}OEt)Cl_2$ complex. The x-ray structure,

shown in Figure 23, shows $ReO(dpk\text{-}OEt)Cl_2$ to be a distorted octahedron, as the bond angle between the oxo, rhenium center, and singly-bonded oxygen is 156.7°.[32] The Re-oxo bond length is 1.69 Å, indicative of a strong π interaction. The Re-O bond length of 1.98 Å is consistent with a Re-O singly-bonded oxygen.

This complex is both similar and different to $Re(Py_2NO)Cl_3$ as a metallointercalator intermediate. Like $Re(Py_2NO)Cl_3$, the supporting group of $ReO(dpk\text{-}OEt)Cl_2$ is tridentate, binding to three of the six open binding sites on the rhenium metal. This shared nature of the binding of the supporting group makes $ReO(dpk\text{-}OEt)Cl_2$ a viable candidate for a metallointercalator.

Conversely, $ReO(dpk\text{-}OEt)Cl_2$ is different in that it is an oxo complex: a metal complex in which a single oxygen atom forms a double-bond with a metal. This complex differs from the originally proposed $[Re(Py_2NO)(H_2O)dppz]^{3+}$ in that the H_2O molecule can be more easily substituted with other substituent groups than the oxygen atom. This will likely affect the range of DNA binding behaviors that $[ReO(dpk\text{-}OEt)dppz]^{2+}$ will possess, since the oxygen atom has a high binding affinity to the rhenium metal, and thus will be more difficult to substitute with other groups in order to alter the DNA binding behavior of the complex. This does not, however, render $[ReO(dpk\text{-}OEt)dppz]^{2+}$ useless as a metallointercalator. The doubly-bonded oxygen atom will be able to exhibit hydrogen bonding with base pairs in the major and minor grooves of DNA. There have also been no reports of a metallointercalator complex containing an oxo, which would render $[ReO(dpk\text{-}OEt)dppz]^{2+}$ the first representative of a novel class of metallointercalators.

Synthesis of $[ReO(dpk\text{-}OEt)dppz]^{2+}$

$ReO(dpk\text{-}OEt)Cl_2$ was then refluxed with Ag^+ and dppz in acetonitrile in an attempt to synthesize the metallointercalator $[ReO(dpk\text{-}OEt)dppz]^{2+}$ (Fig. 24). After the AgCl precipitate was filtered off, addition of saturated aqueous KPF_6 solution to the reaction filtrate yielded a red/brown solid. An IR spectrum of the crude product shows similarities between the vibrations of the $ReO(dpk\text{-}OEt)Cl_2$ intermediate and the product believed to be $[ReO(dpk\text{-}OEt)dppz][PF_6]_2$. Major vibrations shifted by 50 cm^{-1} or less between the two spectra, suggesting that the dpk-OEt

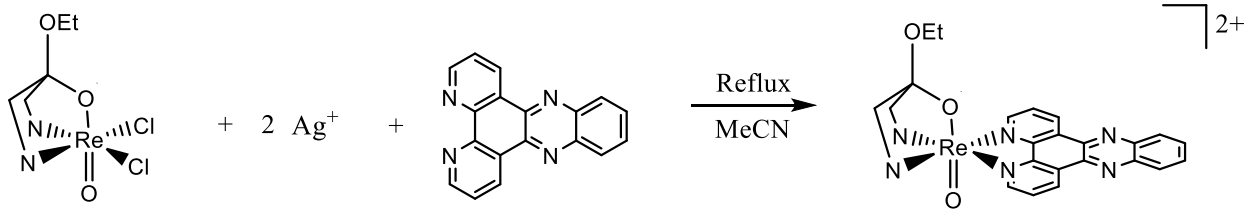

Figure 24: Chemical reaction of $ReO(dpk\text{-}OEt)Cl_2$, silver trifluoromethanesulfonate, and dppz in acetonitrile to produce the metallointercalator $[ReO(dpk\text{-}OEt)dppz]^{2+}$.

ligand remained intact and that dppz is coordinated to the two open binding sites previously occupied by the halide atoms. In addition, a vibration at 829 cm^{-1} is present, which corresponds to the PF_6^- counterion. This value is shifted roughly 20 cm^{-1} from the P-F stretch corresponding to a sample of KPF_6, strongly suggesting that PF_6^- is present in the sample as an anion. Electronic absorption data shows peaks which are similar in structure between the $ReO(dpk\text{-}OEt)Cl_2$ and $[ReO(dpk\text{-}OEt)dppz]^{2+}$ samples (342, 315, and 249 nm and 374, 358, and 277 nm, respectively). These absorptions are shifted 30-40 nm between the samples, which is a promising suggestion that dppz is coordinated to the rhenium metal center.

A ^1H NMR spectrum of the sample shows five resonances in the aromatic region (Fig. 26). Three of these aromatic resonances appear to be triplets and quartets, suggesting hydrogen coupling on the dpk-OEt ligand and dppz. This will be determined through future 2-D NMR

experiments, specifically COSY and HMQC. The $ReO(dpk\text{-}OEt)Cl_2$ resonances in the aromatic region appear to be shifted, which suggests the coordination of dppz to the rhenium metal center, and thus the synthesis of the metallointercalator complex $[ReO(dpk\text{-}OEt)dppz]^{2+}$. The upfield region consists of a triplet at 0.95 ppm, corresponding to the CH_3 protons on the ethoxyl group of dpk-OEt, and a small resonance at 3.05 ppm which is likely a quartet associated with the CH_2 protons of the ethoxyl group. These signals are less pronounced than the ethoxyl group signals in Figure 23, which suggests that this group may have the ability to reversibly add to and leave the carbonyl carbon, forming free ethanol.

The reversible nature of the interaction of di-2-pyridyl ketone and ethanol can be seen in the isolation of a di-rhenium byproduct from the reaction of $ReO(dpk\text{-}OEt)Cl_2$ with silver and dppz. A preliminary crystal structure of this byproduct (Fig. 25) reveals an edge-sharing bioctahedral structure where two Re^{III} centers are bridged by a chloride and an oxo group. One of the rhenium centers is coordinated by a tridentate dpk-OEt group, while the second rhenium center is supported by a bidentate di-2-pyridyl ketone ligand. The two rhenium centers are separated by 2.494 Å

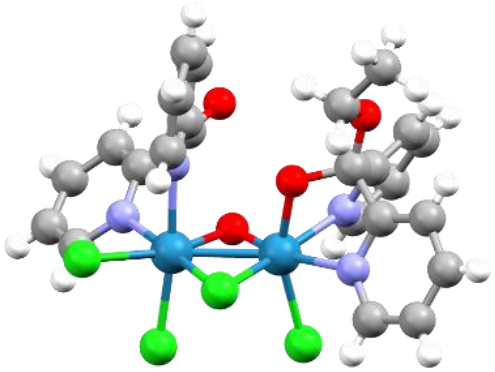

Figure 25: X-ray crystal structure of a di-rhenium byproduct. The byproduct is a Re^{III}-Re^{III} dimer with a bridging oxygen and a bridging chloride, shown in red and green, respectively. Dpk is shown as a ligand on one of the rhenium centers, while dpk-OEt is shown as a ligand on the other rhenium center. Rhenium, Oxygen, Chlorine, Nitrogen, Carbon, Hydrogen (White).

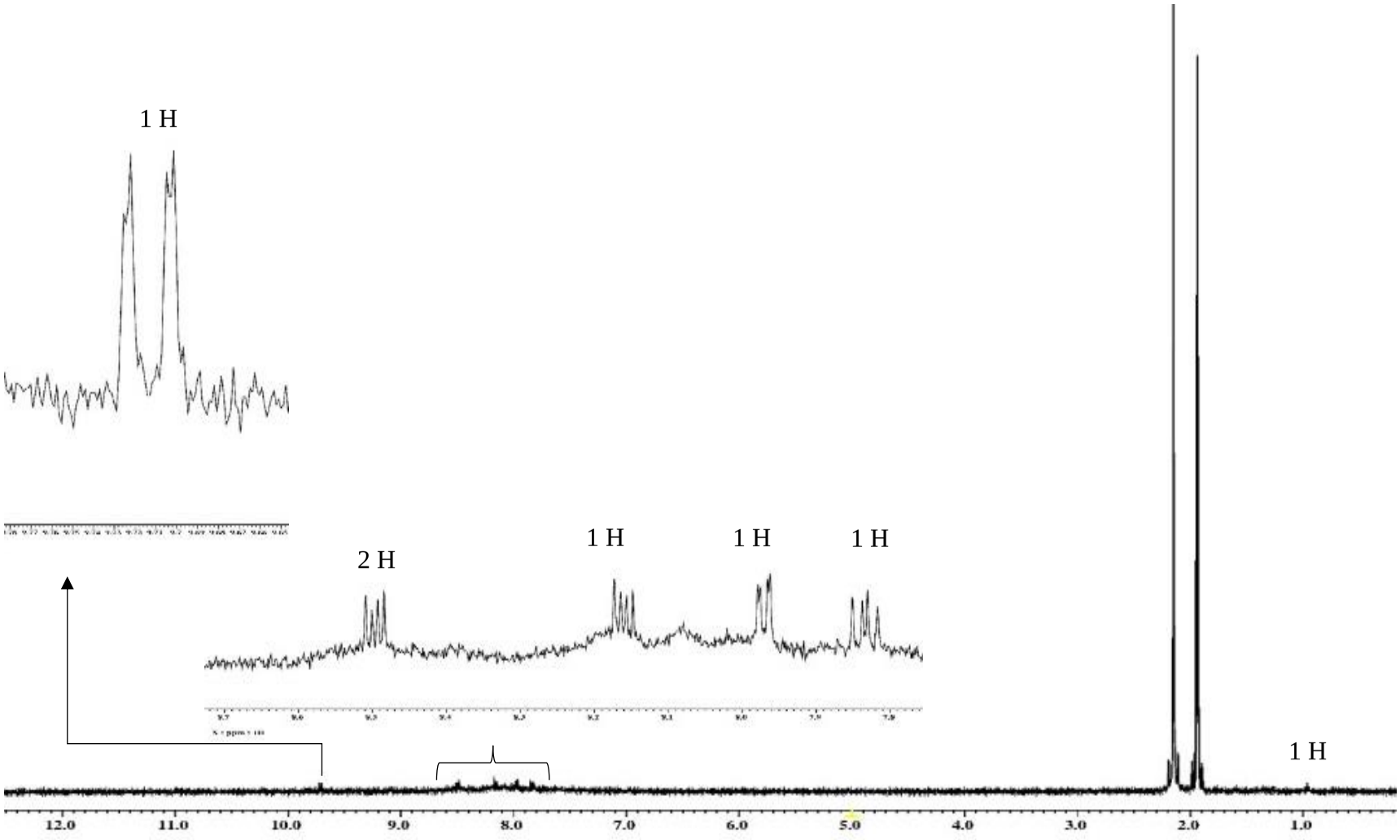

Figure 26: NMR spectrum of the metal complex believed to be [ReO(dpk-OEt)dppz][PF_6]$_2$ (with integration)in deuterated acetonitrile. The splitting shown in the enlarged aromatic region (9-6.5ppm) has shifted slightly from Figure 2, suggesting a change in coordination. Another signal in the aromatic region at 9.7 ppm is enlarged. The increased number of peaks also suggest the presence of another aromatic compound coordinated with the metal center, most likely dppz.

Conclusions

We are continuing to work toward obtaining $Re(Py_2NO)Cl_3$ as a crystalline product, after having discovered a synthesis method which yields a solid product. We have also synthesized the metallointercalator intermediate $ReO(dpk\text{-}OEt)Cl_2$ through a novel synthesis method which produced higher yields than the literature had reported. This complex was then reacted with Ag^+ and dppz in an attempt to produce the metallointercalator $[ReO(dpk\text{-}OEt)dppz]^{2+}$. A solid product precipitated as a PF_6^- salt, which is believed to be the desired metallointercalator. All products have been characterized by IR, NMR, and UV/Vis spectroscopy, and x-ray diffraction studies have been conducted on single crystal samples. Attempts to obtain the metallointercalator $[ReO(dpk\text{-}OEt)dppz]^{2+}$ are ongoing.

Future work will consist of obtaining crystals of both $Re(Py_2NO)Cl_3$ and $[ReO(dpk\text{-}OEt)dppz]^{2+}$ for X-ray diffraction studies. Further syntheses will also attempt to increase the yield of $Re(Py_2NO)Cl_3$. Upon X-ray diffraction studies of $Re(Py_2NO)Cl_3$, further syntheses will attempt to produce the metallointercalator $[Re(Py_2NO)(H_2O)dppz]^{3+}$ using dppz and Ag^+ salts. Upon X-ray diffraction studies of $[ReO(dpk\text{-}OEt)dppz]^{2+}$, DNA binding studies will be commenced in collaboration with Dr. Thayaparan Paramanathan of the Department of Physics at Bridgewater State University in order to achieve the ultimate goal of this project: to understand how these metallointercalators interact with DNA, and to determine their viability as DNA damage probes.

References

(1) Yakovchuk, P.; Protozanova, E.; Frank-Kamenetskii, M. . Base-Stacking and Base Pairing Contributions into Thermal Stability of the DNA Double-Helix. *Nucleic Acids Res.* **2006**, *34*, 564–574.

(2) Kamaraj, B.; Bogaerts, A. Structure and Function of P53-DNA Complexes with Inactivation and Rescue Mutations: A Molecular Dynamics Simulation Study. *PLoS* **2015**, *10*, 1–16.

(3) Jackson, S. P.; Bartek, J. The DNA-Damage Response in Human Biology and Disease. *Nature* **2009**, *461*, 1071–1078.

(4) Russell, P. J. *IGenetics: A Molecular Approach*, 3rd ed.; Pearson: San Francisco, CA, 2010.

(5) Hart, J. R.; Glebov, O.; Ernst, R. J.; Kirsch, I. R.; Barton, J. K. DNA Mismatch-Specific Targeting and Hypersensitivity of Mismatch-Repair-Deficient Cells to Bulky Rhodium(III) Intercalators. *PNAS* **2006**, *103* (42), 15359–15363.

(6) Ernst, R. J.; Komor, A. C.; Barton, J. K. Selective Cytotoxicity of Rhodium Metalloinsertors in Mismatch Repair-Deficient Cells. *Biochemistry* **2011**, *50*, 10919–10928.

(7) Fink, D.; Aebi, S.; Howell, S. B. The Role of DNA Mismatch Repair in Drug Resistance1. *Clin. Cancer Res.* **1998**, *4*, 1–6.

(8) Waywell, P.; Gonzalez, V.; Gill, M. R.; Adams, H.; Meijer, A. J. H. M.; Williamson, M. P.; Thomas, J. A. Structure of the Complex of [Ru (Tpm)(Dppz)Py]2+with a B-DNA Oligonucleotide-A Single-Substituent Binding Switch for a Metallo- Intercalator. *Chem. - A Eur. J.* **2010**, *16*, 2407–2417.

(9) Friedman, A. E.; Chambron, J. C.; Sauvage, J. P.; Turro, N. J.; Barton, J. K. A Molecular Light Switch for DNA: [Ru(Bpy)2(Dppz)]2+. *J. Am. Chem. Soc.* **1990**, *112*, 4960–4962.

(10) Zeglis, B. M.; Pierre, V. C.; Barton, J. K. Metallo-Intercalators and Metallo-Insertors. *Chem. Commun.* **2007**, No. 44, 4549–4696.

(11) Sitlani, A.; Long, E. C.; Pyle, A. M.; Barton, J. K. DNA Photocleavage by Phenanthrenequinone Diimine Complexes of Rhodium(III): Shape-Selective Recognition and Reaction. *J. Am. Chem. Soc.* **1992**, *114*, 2303–2312.

(12) Stoeffler, H. D.; Thorntor, N. B.; Temkin, S. L.; Schanze, K. S. Unusual Photophysics of a Rhenium(I) Dipyridophenazine Complex in Homogenous Solution and Bound to DNA. *J. Am. Chem. Soc.* **1995**, *117*, 7119–7128.

(13) Metcalfe, C.; Webb, M.; Thomas, J. A. A Facile Synthetic Route to Bimetallic ReIcomplexes Containing Two Dppz DNA Intercalating Ligands. *Chem. Commun.* **2002**, 2026–2027.

(14) Aliyan, A.; Kirby, B.; Pennington, C.; Martí, A. A. Unprecedented Dual Light-Switching Response of a Metal Dipyridophenazine Complex toward Amyloid-β Aggregation. *J. Am.*

Chem. Soc. **2016**, *138*, 8686–8689.

(15) Komor, A. C.; Barton, J. K. The Path for Metal Complexes to a DNA Target. *Chem. Commun.* **2013**, *49* (35), 3603–3710.

(16) Odom, D. T.; Parker, C. S.; Barton, J. K. Site-Specific Inhibition of Transcription Factor Binding to DNA by a Metallointercalator. *Biochemistry* **1999**, *38*, 5155–5163.

(17) Jackson, B. A.; Alekseyev, V. Y.; Barton, J. K. A Versatile Mismatch Recognition Agent: Specific Cleavage of a Plasmid DNA at a Single Base Mispair. *Biochemistry* **1999**, *38* (15), 4655–4662.

(18) Nováková, O.; Kašpárková, J.; Vrána, O.; van Vliet, P. M.; Reedijk, J.; Brabec, V. Correlation between Cytotoxicity and DNA Binding of Polypyridyl Ruthenium Complexes. *Biochemistry* **1995**, *34*, 12369–12378.

(19) Gill, M. R.; Thomas, J. A. Ruthenium(Ii) Polypyridyl Complexes and DNA - From Structural Probes to Cellular Imaging and Therapeutics. *Chem. Soc. Rev.* **2012**, *41*, 3179–3192.

(20) Ali Nazif, M.; Bangert, J. A.; Ott, I.; Gust, R.; Stoll, R.; Sheldrick, W. S. Dinuclear Organoiridium(III) Mono- and Bis-Intercalators with Rigid Bridging Ligands: Synthesis, Cytotoxicity and DNA Binding. *J. Inorg. Biochem.* **2009**, *103*, 1405–1414.

(21) Geldmacher, Y.; Oleszak, M.; Sheldrick, W. S. Inorganica Chimica Acta Rhodium (III) and Iridium (III) Complexes as Anticancer Agents. *Inorganica Chim. Acta* **2012**, *393*, 84–102.

(22) Williams, I. M.; Hancock, H. L.; Haefner, S. C. *DNA Binding Studies of [Rh(Tacn)(Dppz)(H2O)]3+: A New Metallointercalator With A Modifiable Coordination Site*; 2015.

(23) Hancock, H. L.; Haefner, S. C. *Synthesis and Characterization of 1,4,7-Triazacyclononane (Tacn) Based Rh(III) Metallointercallators*; 2013.

(24) Pham, M.; Haefner, S. C. *Synthesis and Characterization of [Ru(Tacn)(Dppz)(H2O)]2+: A New Potential Metallointercalator*; 2013.

(25) Culcu, G.; Haefner, S. C. *Investigations into the Synthesis of [Ir(Tacn)(Dppz)(H2O)]3+: A New Potential Metallointercalator for DNA Binding*; 2014.

(26) Ito, A.; Nakano, Y.; Urabe, M.; Tanaka, K.; Shiro, M. Structural and Magnetic Studies of Copper(II) and Zinc(II) Coordination Complexes Containing Nitroxide Radicals as Chelating Ligands. *Eur. J. Inorg. Chem.* **2006**, 3359–3368.

(27) Gass, I. A.; Tewary, S.; Rajaraman, G.; Asadi, M.; Lupton, D. W.; Moubaraki, B.; Chastanet, G.; Le, J.; Murray, K. S. Solvate-Dependent Spin Crossover and Exchange in Cobalt(II) Oxazolidine Nitroxide Chelates. *Inorg. Chem.* **2014**, *53*, 5055–5066.

(28) Gass, I. A.; Asadi, B. M.; Lupton, A. D. W.; Moubaraki, A. B.; Bond, A. M.; Guo, A. S.; A, K. S. M. Manganese (II) Oxazolidine Nitroxide Chelates : Structure , Magnetism , and Redox Properties. *Aust. J. Chem.* **2014**, *67*, 1618–1624.

(29) Gass, I. A.; Gartshore, C. J.; Lupton, D. W.; Moubaraki, B.; Nafady, A.; Bond, A. M.; Boas, J. F.; Cashion, J. D.; Milsmann, C.; Wieghardt, K.; et al. Anion Dependent Redox Changes in Iron Bis-Terdentate Nitroxide { NNO } Chelates. *Inorg. Chem.* **2011**, *50*, 3052–3064.

(30) Gass, I. A.; Tewary, S.; Nafady, A.; Chilton, N. F.; Gartshore, C. J.; Asadi, M.; Lupton, D. W.; Moubaraki, B.; Bond, A. M.; Boas, J. F.; et al. Observation of Ferromagnetic Exchange , Spin Crossover , Reductively Induced Oxidation , and Field-Induced Slow Magnetic Relaxation in Monomeric Cobalt Nitroxides. *Inorg. Chem.* **2013**, *52*, 7557–7572.

(31) Maverick, A. W.; Hammer, R. P.; Arnold, J. A.; Walton, R. A.; Sattelberger, A. P.; McDonald, L. T.; Lane, S. M.; Haefner, S. C. No Title. *Inorg. Synth.* **2014**, *36*, 223–228.

(32) Pejo, C.; Pardo, H.; Mombrú, A.; Cerdá, M. F.; Gancheff, J. S.; Chiozzone, R.; González, R. Re(V) Complexes Formed by Metal-Assisted Solvolysis of Di-(2-Pyridyl) Ketone: Synthesis, X-Ray Studies, Redox Behavior and DFT Calculations. *Inorganica Chim. Acta* **2011**, No. 376, 105–111.